ISSN: 2639-7536

Research article

Petroleum and Chemical Industry International

Comparative Study of Adhesive Elastoplastic Model Between LIGGGHTS Software and EDEM Software

Maheandar Manokaran* **and Martin Morgeneyer**

Genie de procedes Industriels, Universite de Technologie de Compiegne (UTC), Compiegne, France

***Corresponding Author**
Maheandar Manokaran, Genie de procedes Industriels, Universite de Technologie de Compiegne (UTC), Compiegne, France

Submitted: 2024, May 10; **Accepted**: 2024, Jun 03; **Published**: 2024, Jun 21

Citation: Manokaran, M., Morgeneyer, M. (2024). Comparative Study of Adhesive Elastoplastic Model Between LIGGGHTS Software and EDEM Software. *Petro Chem Indus Intern, 7*(2), 01-07.

Abstract

As of late, the Discrete Element Method (DEM) has been generally used to focus on the complex behavior of granular materials. To apply the model accurately at the individual particle level, it is necessary to determine the model parameters at the particle level and consider the complexities of interfacial interactions. DEM models commonly used to model adhesions, such as JKR, DMT, linear cohesion models, elastoplastic models etc. There are lot of models are implemented in both open source and commercial software. One of the model is Adhesive elastoplastic model, which was implemented in commercial software EDEM. To create a user friendly and application demand, we implemented the same model in Open source software LIGGGHTS. In this work, an adhesive elastoplastic contact (DEM) model for the mesoscopic level with 3D non-spherical particles is implemented in LIGGGHTS,fully target on accomplishing cohesive powder flowability.This model has undergone simulations involving uniaxial compression followed until failure. The contact model utilized in these simulations has been assessed against experimental data, specifically the flow function and compared with results obtained through EDEM simulations for limestone powder (ESKAL), chosen as a benchmark material for comprehensive analysis.The prediction of this work gives the deeper insights of cohesively in the form of contact plasticity and it is key parameter for the behavior of cohesive granular material. This outcomes gives a new opportunity for the user to use the model in open source depend upon their application and as wells the behavior of cohesive granular material.

Keywords: Elasto-Plastic, DEM, Non-Spherical Particles

Abbreviations:

d_{avg}	average particle diameter (m)
e	co-efficient of restitution
F_a	average adhesive strength at contact (N)
f_0	constant adhesive strength at first contact(N)
I_i	moment of inertia (m^4)
k_1	loading stiffness parameter (kN/m)
$k2$	unloading/reloading stiffness parameter (kN/m)
k_a	adhesive stiffness parameter (kN/m)
k_t	tangential stiffness (kN/m)
m^*	equivalent mass of the particles (kg)
N	number of particles
P	Pressure (kPa)
Zi	Instantaneous coordination number
u	unconfined yield strength (kPa)
σ_a	axial stress (kPa)
σ_t	bulk tensile strength (kPa)

σ_1	axial consolidation stress (kPa)
ρ	particle density (kg/m^3)
P_b	bulk density, (kg/m^3)
ε	total bulk deformation
ε_p	total plastic deformation
ϕ	angle of friction (°)
δ	total normal overlap (m)
δ_{max}	maximum normal overlap (m)
δ_p	plastic overlap (m)
η	sample bulk porosity
η_c	consolidated bulk porosity
τ_i	total applied torque (N m)
λ_p	Contact plasticity

1. Introduction

Powders and particulate solids are stored and handled in enormous amounts in different ventures. These solids frequently experience handling and stockpiling challenges that are brought about by the material cohesion. For example, chimney may form, as a consequence of core flow. When the particles agglomerate close to the circumference of the silo, flow only occurs from the center. And, if the product tends to transform it can solidify more and more, ending up with a chimney formation, also called ratholing. The flowability of cohesive solids is indicated using the flow function introduced by Jenike which describes the unconfined strength as a function of the consolidation stress[1]. The flow function of a cohesive solid thusthe important material property for ascientific based design of the needed powder handling devices. Different direct shear tests exist, such as the Jenike circular cell and the Carr–Walker or Schulze annular ring cell but also indirect uniaxial shear tests can be used to evaluate the flowability for a cohesive material [2-8].Indirect uni-axial compression process is employed in this case. The material used for this work is limestone powder for the two varieties ESKAL 500 and ESKAL 300. Several discrete element method (DEM) investigations have been carried out to explore the characteristics of cohesive materials through the utilization of contact models.

Among these, the JKR and DMT contact models stand out as widely acknowledged and accepted within the field for an elastic sphere with adhesion. A number of elastic contact models including JKR, DMT, Maugis, and Matuttis and Schinnermay not be able to capture the exact cohesive behaviour shown in experiments of cohesive powders[4-14]. Due to the minute contact area between fine particles, even modest forces can induce plastic deformation at these interfaces, leading to a stress behaviour [15]. Hence, it is suggested that considering contact plasticity is crucial for accurately simulating this cohesivity dependency. While the elastoplastic contact models proposed by Thornton and Ning and Tomas offer high realism, their formulations are intricate and implementation can be computationally demanding [16,17]. On the other hand, the elastoplastic and adhesive contact model proposed by Luding and Walton, and Johnson might not capture all the subtle nuances at particle contacts [18,19]. However, these models are simpler to implement, less computationally intensive, and hence more suitable for simulating bulk systems. And then elastoplastic contact model are proposed by Morrissey with both linear and non-linear options (by setting the exponents). In later part, it was implemented in commercial software EDEM [20-22]. Since in order to use as a user friendly, we implemented this elastoplastic model in open source software LIGGGHTS-PUBLIC v3.8 by DCS Computing GmbH (Linz, Austria).The results were compared with the both open source software (LIGGGHTS), commercial software (EDEM) and experiments as well[14]. This study deploys 3D non-spherical particles using a multi-sphere technique as described in which is also being used by many others [23-28].This paper portrays the comparison of open and commercial software's with advancement of a discrete element method (DEM) model coupled for quantitative prediction of powder flow behavior.

2. Implemented Model in LIGGGHTS

The DEM contact model implemented in LIGGGHTS is based on the physical phenomena observed during adhesive contact between micron-sized particles or small aggregates.The proposed contact model is conceptually similar to Luding's, Walton and Johnshon'smodel and Morrissey [19-20,29]. The model includes a nonlinear hysteretic spring model to accommodate elastic-plastic contact deformation, along with an adhesive force component that varies based on the plastic contact deformation. The elasto-plastic contact model was applied for particle-particle interactions. The Hertz Mindlin non-slip contact model was applied for particle-wall interactions.The governing equation of this model were listed in Table 1

Table 1: Governing Equation for the Simulation

Force or Torque	Formula	Annotations
Normal Force	Elasto Plastic Contact Model, (Luding, 2008; Morrissey et al., 2013) $\overrightarrow{F_n} =$ $K_1 \delta^n \quad if\ K_2 (\delta^n - \delta^n{}_0) \geq K_1 \delta$ $K_2 (\delta^n - \delta^n{}_0) \quad if\ K_1 \delta^n \geq K_2 (\delta^n - \delta^n{}_0) \geq -K_a \delta^n$ $K_a \delta^n \quad if - K_a \delta^n \geq K_2 (\delta^n - \delta^n{}_0)$ Hertz- Mindlin non-slip Contact model $\overrightarrow{F_n} = \frac{4}{3} E^* \sqrt{R^*} \overrightarrow{\delta^{n^{3/2}}}$	K_1 Loading Stiffness K_2 Unloading Stiffness K_a Adhesion Stiffness δ normal Overlap δ_0 Contact deformation Overlap E^* Equivalent Young's Modulus F_nNormal Force
Normal damping Force	$\overrightarrow{F_n} = \frac{4}{3} E^* \sqrt{R^*} \overrightarrow{\delta^{n^{3/2}}}$	m* Equivalent mass R* Equivalent radius
Tangential force	$\overrightarrow{F_t}$ = -$S_t \overrightarrow{\delta_t}$	S_n Normal Stiffness F_t Tangential Stiffness
Tangential damping Force	$\overrightarrow{F_n^d}$ = -2 $\sqrt{\frac{5}{6}} \beta \sqrt{S_t} m^* \overrightarrow{V_t^{rel}}$	$\overrightarrow{V_t^{rel}}$ relative tangential velocity β damping coefficient
Rolling Torque	$\tau = -\mu_r \overrightarrow{F_n} \frac{\omega}{\lvert\omega\rvert}$	τ Rolling torque ω Relative angular velocity μ_r Rolling Friction Coefficient

2.1Numerical Simulation Setup

An open source software LIGGGHTS-PUBLIC v3.8 by DCS Computing GmbH (Linz, Austria) was used as the simulation software for this work. The uni-axial experiements are simulated by using DEM. The elastoplastic contact model was only applied to particle-particle interaction. For the boundary interaction, Hertz-Mindlin (no-slip) contact model was used. In this, all the particles are non-sphericalparticles with comprises of 2 to 5 paired spheres. All other parameter was chosen appropriately to avoid computational cost, time and particle overlap. The setup of the uni-axial simulation consists of cylindrical shape, with two plates (one with moving and other not moving) Table 2. The process of the simulation is as follows; filling with particles to create aninitial packing after that, stress level is applied to compressed the particle followed by uncompressing. The above process is repeateduntil the particle starts to fail. The same initialpacking is used for all the stress level used in this simulation. During compressing and uncompressing, enough time will provide in order to particle allow to settle.

Table 2: Simulation Parameter Settings

Parameter	Symbol	Value	Note
Number of Particle	-	50000	Based on Computation time
Particle Name, ESKAL 500 & ESKAL 300	-	-	-
Median Particle Size d_{50}	µm	4.42, 2.22	Based on Experimental data [14]
Moisture Content	-	0.9, 0.9	Based on Experimental data [14]
Initial bulk density	ρ_{bo} (kg/m^3)	730, 540	Based on Experimental data [14]
Particle Density	ρ (kg/m^3)	2300	Based on Experimental data [14]
Coefficient of restitution	e	0.4	Particle to particle and to wall
Particle Static Friction	μ_{sf}	0.5	Based on Powder flow simulation
Particle Rolling Friction	μ_{rf}	0.001	Based on powder flow simulation
Wall Friction	μ_{wf}	0	-
Top and bottom plate friction	μ_{pf}	0.1	-
Platen Speed	(s^{-1})	0.5	-

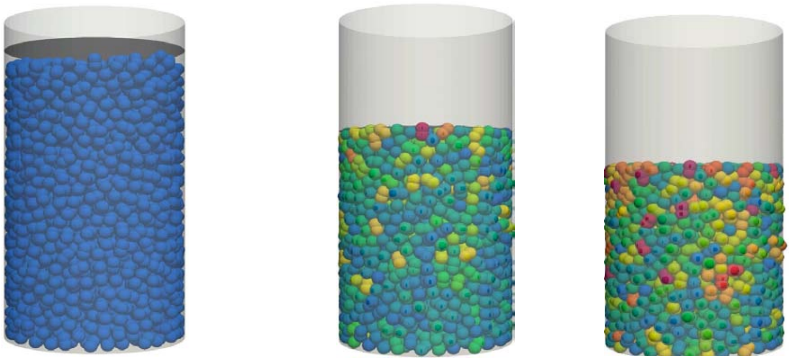

Figure 1: Images of Uniaxial Test Simulations: (a) Filling, (b) Confined Consolidation, and (c) Unconfined Compression

To ensure the system stabilized, loading only began when the ratio of kinetic to potential energy dropped below 10^-5, maintaining a consistent coordination number. The process involved compressing the sample vertically by lowering the top platen at a steady strain rate. Once the desired stress was reached, the load was released by raising the top platen at the same rate. Subsequently, the lateral confining walls were removed, allowing the unconfined sample to relax briefly. This allowed the dissipation of kinetic energy resulting from removing the confining walls and lifting the top platen. Following this, the sample was compressed to failure by lowering the top platen again at a constant rate. The same process and methods are employed in both EDEM and experiments as well.

3. Results and Discussion

One of the key areas in this elastoplastic model, it can able to predict the flow behaviour of powder under different consolidation stresses. The graphs **(Figure 2** and **Figure 3)** shows the predicted flow function of limestone powder (ESKAL 500 and ESKAL 300). The graph **(Figure 2)** was plotted between axial consolidation stresses against flow function for ESKAL 500. For the boundaries chose, the implemented model anticipated that is in good quantitative understanding with the experimental as well EDEM outcomes. And also the results of JKR with an elastic Hertizan contact in the LIGGGHTS code version 3.8 is also plotted in the **Figure 2** [32]. Similarly, for ESKAL 300 the graph **(Figure 3)** was plotted between axial consolidation stresses against flow function.

In this case, you can see the good quantitative understanding between experiments and EDEM rather the simulation output generated using LIGGGHTS. The outcomes displayed in Figure 2 and Figure 3 demonstrates that the carried out model is equipped for catching the remarkable highlights of a strong cohesive powder.

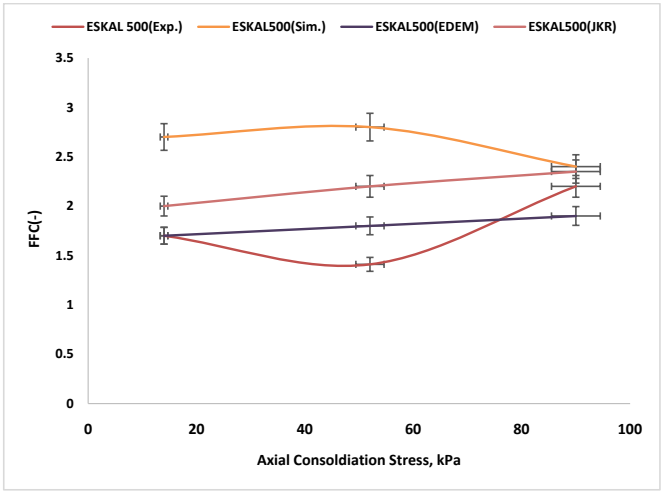

Figure 2 : Axial Consolidation Stress Vs Flow Function for ESKAL 500

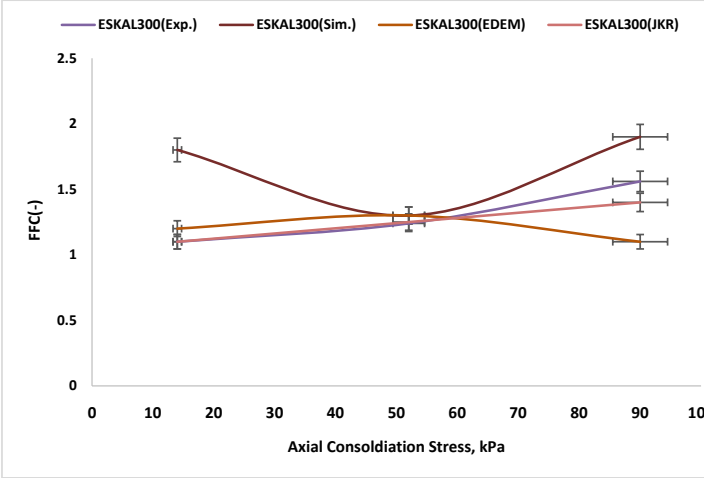

Figure 3: Axial Consolidation Stress Vs Flow Function for ESKAL 300

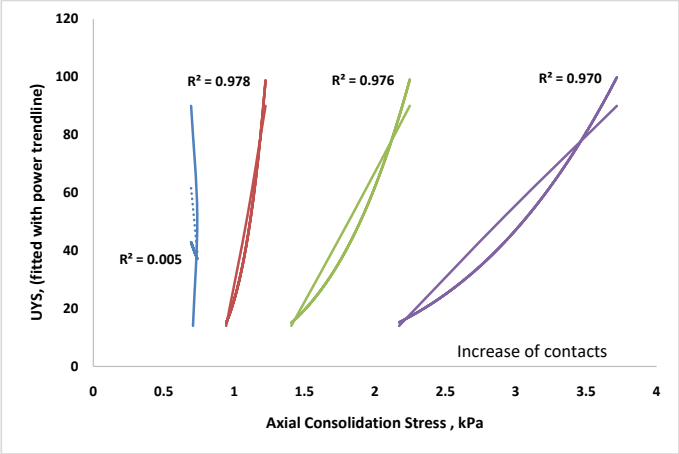

Figure 4:Axial Consolidation Stress Vs UYC with Function of Power Trend Line

The model anticipates the origin of the cohesive strength in a micromechanical perspective point of view. One of key relationship in bulk material is contact plasticity. This key parameter shows the key difference in elastic and cohesive contact models. The graph plotted between axial consolidations stresses with unconfined yield strength (fitted with power trend line). From the figure as you can see the when the contact plasticity level is increasing, the line starts to become bit by bit angular. This power trend line (i.e. a straight line that minimizes the distance between it and some data) shows the when there is small level of contact plasticity, the line is straight. In other way if we plot the slope function, we can see the continues increase of slope value. These values or range indicated the level of cohesion between the particles. Based on these, more the contact plasticity, which leads to more contact between the particle leads the cohesive. Theoretically [21,33] the level of bulk cohesion can increase from two sources: increasing the number of inter-particle contacts (i.e. the coordination number) and increasing the respective inter-particle contact forces (e.g. by flattening of the contact under loading). It is clear that the flow function is firmly subject to the contact plasticity.

4. Conclusion

DEM simulation and micromechanical analysis of cohesive powder utilizing an adhesive elasto-plastic contact model was introduced. Adhesive elastoplastic contact model was implemented in open-source software LIGGGHTS. The results of the flow function for ESKAL500, 300 was compared with experiments and commercial software EDEM.The outcomes showed that the model was able to capture the flow function of powder, as observed in the experiment. In short, the findings confirm that the elasto-plastic adhesive model is suitable to simulate cohesive solids exposed to different stress regimes. The plasticity of particle contact has been shown to be essential for capturing stress history dependencies and generating realistic flow functions. Micromechanical analysis reveals that increasing the plasticity of particle contact increases the plasticity of the bulk. Contact plasticity prevents excessive elastic rebound at the contact surface and reduces porosity when loaded. The effect of adhesion parameters, influence of DEM parameters and time dependency will be the key areas to work in the future [30-31].

Acknowledgment

This project has received funding from the European Union's Horizon 2020 research and innovation program under the Marie Skłodowska-Curie grant agreement No. 812638 (CALIPER).

Reference

1. Jenike, A. W. (1964). Storage and flow of solids. *Bulletin No. 123, Utah State University*.
2. Carr, J. F., & Walker, D. M. (1968). An annular shear cell for granular materials. *Powder Technology, 1*(6), 369-373.
3. Schulze, D. (2010). Flow properties of powders and bulk solids (fundamentals). *Powder Technol, 65,* 321-333.
4. Bell, T. A., Catalano, E. J., Zhong, Z., Ooi, J. Y., & Rotter, J. M. (2007). Evaluation of the Edinburgh powder tester. *Proceedings of PARTEC, Nuremburg, Germany*.
5. Enstad, G. G., & Ose, S. (2003). Uniaxial testing and the performance of a pallet press. *Chemical Engineering & Technology: Industrial Chemistry-Plant Equipment-Process Engineering-Biotechnology, 26*(2), 171-176.
6. Freeman, R., & Fu, X. (2011). The development of a compact uniaxial tester. *Part. Sci. Anal. Edinburgh, UK*, 1-6.
7. Parrella, L., Barletta, D., Boerefijn, R., & Poletto, M. (2008). Comparison between a uniaxial compaction tester and a shear tester for the characterization of powder flowability. *KONA Powder and particle Journal, 26*, 178-189.
8. Williams, J. C., Birks, A. H., & Bhattacharya, D. (1971). The direct measurement of the failure function of a cohesive powder. *Powder Technology, 4*(6), 328-337.
9. Johnson, K. L., Kendall, K., & Roberts, A. A. D. (1971). Surface energy and the contact of elastic solids. *Proceedings of the royal society of London. A. mathematical and physical sciences, 324*(1558), 301-313.
10. Derjaguin, B. V., Muller, V. M., & Toporov, Y. P. (1975). Effect of contact deformations on the adhesion of particles. *Journal of Colloid and interface science, 53*(2), 314-326.
11. Maugis, D. (1992). Adhesion of spheres: the JKR-DMT transition using a Dugdale model. *Journal of colloid and interface science, 150*(1), 243-269.
12. Matuttis, H. G., & Schinner, A. (2001). Particle simulation of cohesive granular materials. *International Journal of Modern Physics C, 12*(07), 1011-1021.
13. Röck, M., Ostendorf, M., & Schwedes, J. (2006). Development of an uniaxial caking tester. *Chemical Engineering & Technology: Industrial Chemistry-Plant Equipment-Process Engineering-Biotechnology, 29*(6), 679-685.
14. Morgeneyer, M., Röck, M., Schwedes, J., Johnson, K., Kadau, D., Wolf, D. E., & Heim, L. (2005). Microscopic and macroscopic compaction of cohesive powders. *Powders and Grains, 535*.
15. Tomas, J. (2007). Adhesion of ultrafine particles—a micromechanical approach. *Chemical Engineering Science, 62*(7), 1997-2010.
16. Thornton, C., & Ning, Z. (1998). A theoretical model for the stick/bounce behaviour of adhesive, elastic-plastic spheres. *Powder technology, 99*(2), 154-162.
17. Tomas, J. (2001). Assessment of mechanical properties of cohesive particulate solids. Part 1: Particle contact constitutive model. *Particulate science and technology, 19*(2), 95-110.
18. Luding, S. (2008). Cohesive, frictional powders: contact models for tension. *Granular matter, 10*(4), 235-246.
19. Walton, O. R., & Johnson, S. M. (2009, June). Simulating the effects of interparticle cohesion in micron-scale powders. In *AIP conference proceedings* (Vol. 1145, No. 1, pp. 897-900). American Institute of Physics.
20. Morrissey, J. P. (2013). Discrete element modelling of iron ore pellets to include the effects of moisture and fines.
21. Thakur, S. C., Morrissey, J. P., Sun, J., Chen, J. F., & Ooi, J. Y. (2014). Micromechanical analysis of cohesive granular materials using the discrete element method with an adhesive elasto-plastic contact model. *Granular Matter, 16*, 383-400.
22. EDEM, "EDEM [Computer Software] DEM Solutions Ltd." Computer Code, Edinburgh, Scotland, 2022. [Online].

Available: https://www.altair.com
23. Favier, J. F., Abbaspour-Fard, M. H., Kremmer, M., & Raji, A. O. (1999). Shape representation of axi-symmetrical, non-spherical particles in discrete element simulation using multi-element model particles. *Engineering computations, 16*(4), 467-480.
24. Chung, Y. C., & Ooi, J. Y. (2006). Confined compression and rod penetration of a dense granular medium: discrete element modelling and validation. In *Modern trends in geomechanics* (pp. 223-239). Berlin, Heidelberg: Springer Berlin Heidelberg.
25. Härtl, J., & Ooi, J. Y. (2008). Experiments and simulations of direct shear tests: porosity, contact friction and bulk friction. *Granular Matter, 10*, 263-271.
26. Kodam, M., Bharadwaj, R., Curtis, J., Hancock, B., & Wassgren, C. (2009). Force model considerations for glued-sphere discrete element method simulations. *Chemical Engineering Science, 64*(15), 3466-3475.
27. Kruggel-Emden, H., Rickelt, S., Wirtz, S., & Scherer, V. (2008). A study on the validity of the multi-sphere Discrete Element Method. *Powder Technology, 188*(2), 153-165.
28. Thakur, S. C., Ahmadian, H., Sun, J., & Ooi, J. Y. (2014). An experimental and numerical study of packing, compression, and caking behaviour of detergent powders. *Particuology, 12*, 2-12.
29. Luding, S. (2008). Cohesive, frictional powders: contact models for tension. *Granular matter, 10*(4), 235-246.
30. Thakur, S. C. (2014). Mesoscopic discrete element modelling of cohesive powders for bulk handling applications.
31. Sheng, Y., Lawrence, C. J., Briscoe, B. J., & Thornton, C. (2004). Numerical studies of uniaxial powder compaction process by 3D DEM. *Engineering Computations, 21*(2/3/4), 304-317.
32. LIGGGHTS 3.8.0, "LIGGGHTS (Version 3.8.0). [Computer Software] DCS Computing GmbH." 2022.
33. MORGENEYER, M., & SCHWEDES, J. (2003). Investigation of powder properties using alternating strain paths. *Task Quarterly, 7*(4), 571-578.